




Article

Single-Piece All-Solid-State Potential Ion-Selective Electrodes Integrated with Molecularly Imprinted Polymers (MIPs) for Neutral 2,4-Dichlorophenol Assessment

Samar Ezzat ^{1,2}, Mona A. Ahmed ², Abd El-Galil E. Amr ^{3,4,*} , Mohamed A. Al-Omar ³ ,
Ayman H. Kamel ¹  and Nagy M. Khalifa ^{3,4}

¹ Department of Chemistry, Faculty of Science, Ain Shams University, 11566 Cairo, Egypt

² Chemistry Department, College for Women, Ain Shams University, Heliopolis, 11751 Cairo, Egypt

³ Pharmaceutical Chemistry Department, Drug Exploration & Development Chair (DEDC),
College of Pharmacy, King Saud University, Riyadh 11451, Saudi Arabia

⁴ Applied Organic Chemistry Department, National Research Center, 12622 Giza, Egypt

* Correspondence: aamr@ksu.edu.sa; Tel.: +966-565-148-750

Received: 11 August 2019; Accepted: 3 September 2019; Published: 10 September 2019



Abstract: A novel single-piece all-solid-state ion-selective electrode (SC/ISE) based on carbon-screen printed is introduced. Polyaniline (PANI) is dissolved in a membrane cocktail that contains the same components used for making a conventional ion-selective polyvinyl chloride (PVC) matrix membrane. The membrane, having the PANI, is directly drop-casted on a carbon substrate (screen-printed-carbon electrode). PANI was added to act as an intermediary between the substrate and the membrane for the charge transfer process. Under non-equilibrium sensing mechanism, the sensors revealed high sensitivity towards 2,4-dichlorophenol (DCP) over the linearity range 0.47 to 13 μM and a detection limit 0.13 μM . The selectivity was measured by the modified separate solution method (MSSM) and showed good selectivity towards 2,4-DCP over the most commonly studied ions. All measurements were done in 30 mm Tris buffer solution at a pH 5.0. Using constant-current chronopotentiometry, the potential drift for the proposed electrodes was checked. Improvement in the potential stability of the SPE was observed after the addition of PANI in the sensing membrane as compared to the corresponding coated-wire electrode (membrane without PANI). The applicability of the sensor has been checked by measuring 2,4-DCP in different water samples and the results were compared with the standard HPLC method.

Keywords: solid-contact ISEs; molecularly imprinted polymers (MIPs); chlorophenols; 2,4-dichlorophenol; neutral response mechanism.

1. Introduction

Chlorophenols, a class of organic pollutants, have recently drawn considerable attention. These organochlorine compounds have been classified as persistent organic pollutants (POPs) as well as endocrine disrupting compounds (EDCs) [1–3]. Due to their constancy in aquatic environments, they can be released to either surface or ground waters as good as bottom sediments. 2,4-DCP has been widely applied in the yield of various herbicides, pesticides, preservatives, and plant growth regulators [4]. Most of the chlorinated phenols can be found and are accumulated in the human body through the food cycle. They can cause felled effects such as faintness, itch, anemia, and cancer risk at extremely low concentration levels [3,5]. After inhalation of 2,4-DCP, the respiratory tract is irritated and this is harmful to the liver, kidneys and organs forming blood [6–9]. Long exposure to 2,4-DCP can

cause serious effects to the respiratory system in addition to permanent sight failure or blindness [7–10]. The European Union and US Environmental Protection Agency (EPA) have regulated its maximum allowable concentration in water at 0.5 µg/L [11]. Therefore, it is important to introduce fast, rigorous, precise, and cost-effective analytical methods to identify and assess this pollutant.

Recently, different reported methods such as HPLC [12], GC/MS [13,14], chemiluminescence [15,16], capillary electrophoresis [17], and UV spectrophotometry [18] have been established for the assessment of 2,4-DCP. Chlorophenol compounds are electrochemically active because of the phenolic –OH group. So, some electrochemical sensors for the assessment of 2,4-DCP have been also reported [19]. These electrochemical sensors showed some excellent features such as fast response and high sensitivity. However, they exhibit poor selectivity because they are limited to distinguishing 2,4-DCP and other chlorophenols. This can be assigned to the lack of special recognition design.

Molecularly imprinted polymers (MIPs) when integrated with electrochemical sensors have picked up a great attention because of their high selectivity and sensitivity [20–22]. In addition, these artificial receptors have high robustness, good stability towards high temperatures and pressures, high resistance towards chemical changes, cost-effective, and can be re-used without remarkable deterioration [23]. Recently, integration of MIPs with ISEs revealed a success in organics detection [24–26]. Only very few potentiometric sensors for 2,4-DCP determination were reported recently [24,27]. Doping of quaternary ammonium salt in polymeric membranes revealed a super-Nernstian response towards electrically neutral phenolic compounds at neutral pH values. These unexpected anionic responses are due to the net movement of H⁺ ions to the aqueous medium coming from the membrane. These H⁺ were induced after the complexation of neutral phenols with the quaternary ammonium salt present in the sensing membrane [20,23,28].

Nowadays, solid-contact ion-selective electrodes SC/ISEs have drawn important attention for environmental monitoring. In the beginning, they were designed in the form of planar configuration called “screen printed electrodes (SPEs)”. The ion-sensing membranes (ISMs) were drop-casted on the conductive substrate in the platform [29]. However, the ill-defined interface between the ISM and the conductive substrate often causes a drift for the electrode potential [30,31]. Thus, much study has been concentrated on introducing new solid-contact transducers to enhance the performance characteristics of the electrodes. One of these important transducers are conducting polymers (CPs), which are characterized by their high electronic and ionic conductivity [32]. A minimal potential drift can be achieved by inserting the solid-contact material between the sensing membrane and electronic substrate. Conducting polymers (CPs) have redox buffer capacity through their oxidation/reduction. Therefore, they provide an effective ion-to-electron transduction. The response mechanism using these CPs was previously explained by several works [33,34]. The implementation of solid contact materials in the electrode can be done in two ways: (i) modification of the substrate of the electrode as in the case of redox active monolayers and carbon-based materials [35–40]. (ii) By directly dissolving the solid-contact transducer in the sensing membrane cocktail and then is drop-cast on the substrate electrode (i.e., so called “Single-Piece-ISEs”) [41]. The later provides good compatibility between the transducer and the conductive substrate of the electrode [41].

In this work, novel single-piece all solid-contact screen-printed sensors assigned with MIP beads for neutral 2,4-DCP as a persistent organic pollutants (POPs) are prepared and characterized. Polyaniline (PANI) film is used as a solid contact transducer. The MIP beads are used as selective receptors for 2,4-DCP and incorporated into the sensing membrane. The presented screen-printed platforms revealed a high sensitivity for the assessment of 2,4-DCP.

2. Materials and Methods

2.1. Materials and Instruments

“2,4-dichlorophenol (DCP), 2-chlorophenol (CP), methyl methacrylate (MMA), ethylene glycol dimethacrylate (EGDMA), benzoylperoxide (BPO) and acetonitrile were obtained from Sigma-Aldrich

(St. Lois, USA). High molecular weight poly (vinyl chloride) (PVC), dioctyl phthalate (DOP) and tridodecylmethylammonium chloride (TDMACl) were obtained from Fluka AG (Buchs, Switzerland). Tetrahydrofuran (THF) was distilled before use. Aqueous solutions of 2,4-DCP were prepared with freshly de-ionized water (18.2 M Ω cm specific resistance). 30 mM Tris buffer solution of pH 5.0 was used for all subsequent experiments to ensure that 2,4-dichlorophenol is in its de-protonated form”.

“Fourier-transform infrared spectroscopy (FT-IR) measurements were carried out using FT-IR spectrometer (Alpha II, Bruker ABCO, Cairo, Egypt) using the attenuated total reflection (ATR) technique. Impedance and chronopotentiometry measurements of the screen-printed electrodes (SPE) were measured using Metrohm potentiostat/galvanostat (Autolab, model 204) purchased from Metrohm Instruments (Herisau, Switzerland). A three-electrode configuration cell containing Silver/Silver chloride (3 M KCl) reference electrode and an auxiliary electrode made from platinum wire was employed. The spectra of impedance were recorded at open-circuit potential in 0.01 M 2,4-dichlorophenol solution with an excitation amplitude of 10 mV. The frequency range starts from 100 kHz to 0.1 Hz. Chronopotentiometry was done at a constant current of ± 1 nA, applied to the working electrode for 60 s followed by a reversed current for another 60 s. The electrolytic solution for these measurements was 10^{-2} M DCP. All potential measurements were done with an Orion (720/SA pH/mV meter, Cambridge, MA, USA) at 25 ± 1 °C using all-solid-state potential ISEs”.

2.2. Synthesis of MIPs

“2,4-Dichlorophenol was used as a template for 2,4-dichlorophenol (2,4-DCP). The MIP beads were prepared by the precipitation method [42]. The synthesis process involves 1.0 mmol of DCP (template), 3.0 mmol of MMA (monomer) and 3.0 mmol of EGDMA (cross-linker), placed in a 25 mL capped glass tube. The mixture was left for 1 h for pre-complex formation between 2,4-DCP and MMA molecules then dissolved in 15 mL of acetonitrile. A 80 mg of benzoylperoxide (BPO) were added into the mixture and nitrogen gas was used as a purging gas for 10 min under a gentle flow. In an oil bath at 80 °C, the polymerization process was carried for 18 h. After complete polymerization, the polymer obtained was collected by vacuum filtration, grinded, and washed circularly with 200 mL absolute methanol to remove the un-reacted species. Template removal was carried out using methanol/acetic acid (9:1, v/v) mixture and then followed by methanolic wash. The obtained polymer was dried overnight at 50 °C under vacuum. In the absence of a template, the non-imprinted polymer (NIP) was also prepared under the same conditions”.

2.3. Design and Fabrication of the Screen-printed Electrodes (SPEs)

“The design of the screen-printed electrode (SPE) is shown in Figure 1. Both carbon and Ag/AgCl were printed on Alumina substrate of 0.1 mm thickness and 35 mm length. The screen for either carbon or Ag/AgCl ink printing was of 2 mm width. The membrane cocktail of SPEs was prepared by dissolving 100 mg of the components in ~1.5 mL THF as: MIP or NIP beads (9.9 wt %), TDMAC (1.2 wt %), PVC (31.2 wt %), DOP (56.3 wt %) and PANI (1.4%). The reference membrane cocktail was prepared by dissolving 78.1 mg polyvinyl butyral (PVB), 50 mg NaCl in 1 mL methanol. The SPE was rinsed with water and THF before use. 15 μ L of the two different membrane cocktails were drop-casting onto the SPE and reference membrane, respectively and left to dry for 6 h”.

“For comparison, MIP/DCP-ISE were also fabricated from membranes have no PANI, drop-casted on the carbon screen-printed platform. Membrane sensors without PANI were the same as for the respective SPEs. The obtained membranes were of 0.1–0.2 μ m thickness. For non-equilibrium potentiometric detection of de-protonated 2,4-DCP, all electrodes were conditioned for at least 2 h in 30 mM Tris buffer (pH 5)”.

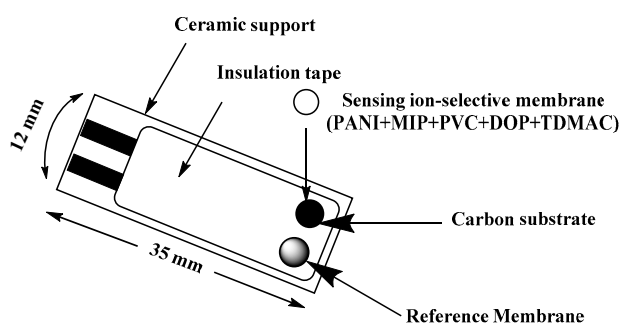


Figure 1. Schematic representation of screen printed planar electrode.

2.4. Potentiometric Measurements

“All potentiometric measurements were performed at 20 ± 1 °C using a digital pH/mV meter (Orion SA 720, Cambridge, MA, USA) with the SPE [or Coated wire electrode (CWE)]. All 2,4-DCP concentrations (1.0×10^{-6} to 1.0×10^{-2} M) were freshly prepared in 30 mm tris buffer (pH5). The electrode potential was measured for each concentration and the resulting EMF values were used for constructing the calibration curve. Selectivity coefficients (K^{pot}_{ij}) were evaluated using the so called “modified separate solution method (MSSM) [43]”.

3. Results and Discussions

3.1. Characterization of the MIP Particles

Polymer characterization has been made by FT-IR spectral analysis to show the imprinting process using MMA monomer through the absence/presence of 2,4-DCP on either washed or non-washed polymer beads. As shown in Figure 2, the spectrum of 2,4-DCP showed a strong medium band assigned to stretching O–H band and located at 3423 cm^{-1} . In addition, sharp and strong peak around 1479 cm^{-1} which is assigned to aromatic ring stretching vibrations. All these assignable peaks clearly appeared in MIP/MMA before the removal of 2,4-DCP and completely disappeared in the spectrum of MIP particles after 2,4-DCP removal. The IR spectrum of MIP/MMA/EGDMA revealed a weak and broad band at 3543 cm^{-1} for νOH stretching and other peaks at 1719 cm^{-1} and 1160 cm^{-1} for $-\text{C}=\text{O}$ or $-\text{C}-\text{O}$ stretches, respectively, which are commonly present in all IR-spectra because of the use of EGDMA cross-linkers. The $\nu\text{C}=\text{O}$ in both washed MIP and NIP beads was located at 1729 cm^{-1} .

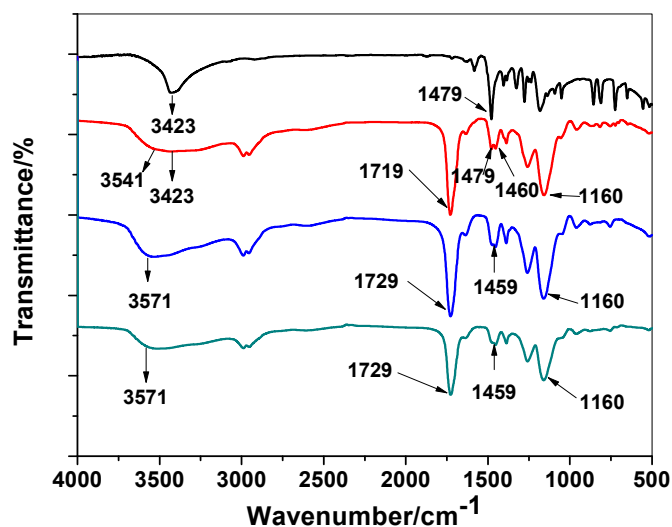


Figure 2. FT-IR spectra for 2,4-Dichlorophenol (DCP), DCP/molecularly imprinted polymers (MIP), MIP/washed and non-imprinted polymer (NIP) beads.

“This shift may be attributed to the contribution of the carbonyl group in the interaction with the DCP molecule. The –O–H stretch outcomes from the methacrylic monomer have a broad peak at 3543 and 3423 cm^{-1} . This peak appeared at 3571 cm^{-1} in both NIP and washed MIP particles and becomes broader. From all of the above, we can prove the possibility of the interaction between the phenolic O–H group and the carbonyl from the carboxylic group of MMA. This confirms the imprinting process of 2,4-DCP using MMA as a functional monomer”.

“The surface of the resulting imprinted MIP beads was analyzed by scanning electron microscopy (SEM) (JOEL, Osaka, Japan). As seen in Figure 3, the DCP imprinted and NIP beads are uniform and spherical in shape with a diameter distribution of 1.2–1.9 μm and 0.43–1.5 μm , respectively. The difference in particle size between MIP and NIP beads can be attributed to the imprinting effect. Because of this size and spherical shape, the obtained beads can be dispersed well in the ISE membrane and revealed high binding capability towards 2,4-DCP. Because of the well dispersion of the beads in the polymeric membrane, more available binding sites in the ISM and thus result in better response performance can be obtained [44]”.

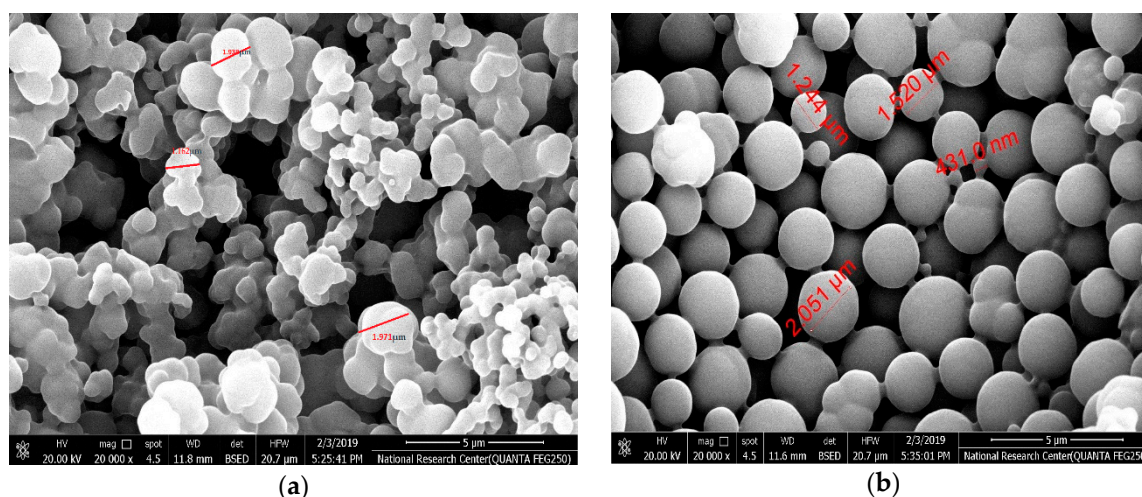


Figure 3. SEM images of (a) MIP and (b) NIP beads.

Binding isotherms and scatchard analyses were performed with different initial 2,4-DCP concentrations at fixed amounts of either MIPs or NIPs micro beads. The mixtures were left until reaching equilibrium and the remaining 2,4-DCP concentrations were evaluated spectrophotometrically at $\lambda_{\text{max}} = 284 \text{ nm}$. The resulting binding capacity (Q) of MIPs was calculated according to following Equation (1):

$$Q = \text{DCP}_{\text{bound}} (\mu\text{mol}/\text{mL}) / \text{MIP} (\text{gm}) = (C_i - C_f) V_s \times 1000 / m_{\text{MIP}} \quad (1)$$

where Q is binding capacity ($\mu\text{mol}/\text{g}$), C_i the initial DCP concentration ($\mu\text{mol}/\text{mL}$), C_f the final DCP concentration ($\mu\text{mol}/\text{ml}$), V_s the volume of tested solution (mL) and m_{MIP} the mass of dried polymer (mg). The calculated binding capacities were used to plot the binding isotherms (Figure 4).

The Scatchard analysis was subsequently used to evaluate the binding characteristics using Equation (2):

$$Q/C_f = (Q_{\text{max}} - Q) / K_d \quad (2)$$

where Q is the binding capacity, C_f is the free DCP concentration at equilibrium ($\mu\text{mol}/\text{mL}$), Q_{max} is the maximum apparent binding capacity, and K_d is the dissociation constant at binding site. As shown in Figure 5a,b, The K_d and Q_{max} for the high affinity binding sites were found to be 416.6 $\mu\text{mol}/\text{L}$ and 264.3 $\mu\text{mol}/\text{g}$ for MIP beads and 163.9 $\mu\text{mol}/\text{L}$ and 45.1 $\mu\text{mol}/\text{g}$ for NIP beads, respectively.

Imprinting factor (IF) is a useful measure of the presence of the template during polymerization, and it is defined in Equation (3):

$$IF = Q_{\text{max}} (\text{MIP}) / Q_{\text{max}} (\text{NIP}) \quad (3)$$

where Q_{max} (MIP) and Q_{max} (NIP) are the bound concentrations on the imprinted and the corresponding non-imprinted polymers, respectively. The imprinting factor (IF) is calculated to be 5.86.

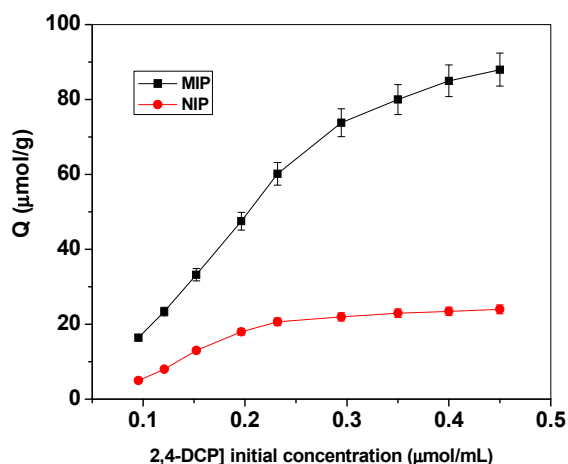


Figure 4. Binding isotherm for MIPs and NIPs. Conditions: 20.0 mg of polymer; $t=25\text{ }^{\circ}\text{C}$; $V=10.0\text{ mL}$.

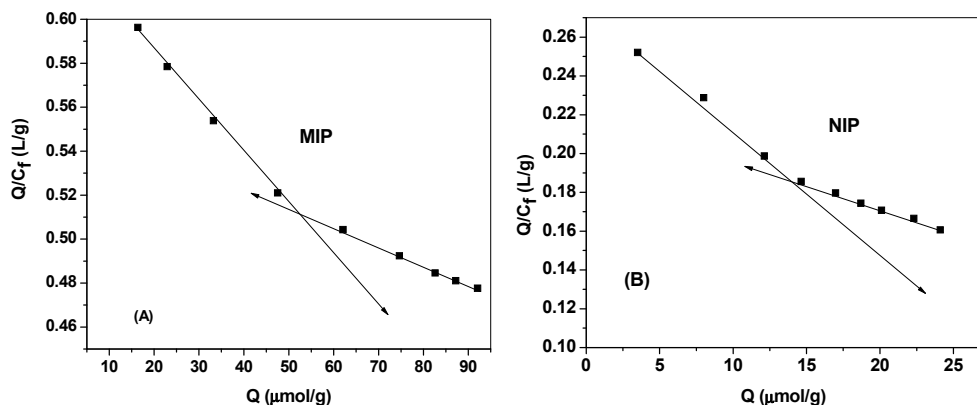


Figure 5. Scatchard plot for (A) MIPs and (B) NIPs. Conditions: 20.0 mg of polymer; $t=25\text{ }^{\circ}\text{C}$; $V=10.0\text{ mL}$.

3.2. Sensor Analytical Features

For a liquid-contact ISE, the membrane sensor is usually conditioned with the primary ion and the potentiometric response is measured under classical equilibrium conditions (30 mM $\text{HCO}_3^-/\text{CO}_3^{2-}$ buffer, pH 10). In our previous work, it was found that phenols in their neutral forms revealed super-Nernstian anionic responses for polymeric membrane potentiometric sensors containing quaternary ammonium salt and MIPs under near-neutral pH conditions [20,45]. These unexpected super-Nernstian anionic behaviors were clarified on the basis of the net movement of H^+ ions from the membrane to the aqueous phase. This movement is stimulated by the association of the neutral phenols with quaternary ammonium salt doped in the sensing membrane. According to these, we applied in this work the concept of the non-classical response in 2,4-dichlorophenol (DCP) detection. To ensure the presence of neutral 2,4-DCP, 30 mM Tris buffer solution of pH 5.0 was used as the solution background. To obtain good sensitivity for the detection of neutral DCP, all experiments were done after the optimization of the experimental factors. From the obtained results, it was found that the sensors revealed the best response behavior and performance after using the non-polar plasticizer DOP. This confirms that neutral 2,4-DCP prefers the DOP solvent to be extracted into the ISM. Figure 6a represents the response of the screen-printed platform in absence/presence of DCP under the optimized conditions. The amount of 2,4-DCP is estimated from the difference in potential between the baseline values and those at a fixed time (i.e., 100 s). At higher concentrations of DCP, we noticed stronger

anionic response due to the more net movements of H^+ from the membrane to the aqueous phase [28]. The obtained results indicated that the electrodes revealed a potential response which is directly dependent on the concentration of neutral DCP. The sensor can detect low level concentration of 2,4-DCP down to $0.13 \mu\text{M}$ within a linearity range starts from 0.47 to $13 \mu\text{M}$.

For comparison, the response of NIP-based membrane sensors towards neutral 2,4-DCP was also recorded. As mentioned in Figure 6b, the potential response of MIP-membrane based sensor revealed higher anionic response than the NIP membrane-based sensor towards the same concentration of DCP (i.e., $2.5 \mu\text{M}$). This can be considered as a proof for the successful imprinting of 2,4-DCP. From all of the data above, we can confirm that low cost screen-printed platforms are an effective alternative to expensive noble metal electrode substrates.

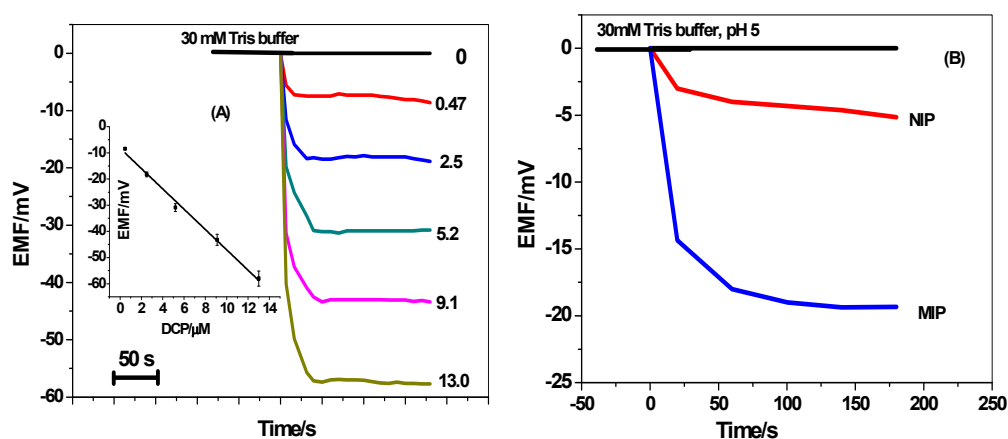


Figure 6. (A) The dynamic potentiometric responses of screen-printed platform towards neutral 2,4-DCP in 30 mM Tris buffer at pH 5. The inset shows the measuring calibration plot for 2,4-DCP; (B) The potential responses to $2.5 \mu\text{M}$ neutral 2,4-DCP using the blank, NIP and MIP based membranes.

3.3. Selectivity

The selectivity of the presented electrodes over other neutral phenols such as 2-chlorophenol, phenol, *p*-cresol, salicylic acid, and other common anions such as Br^- , Cl^- is shown in Figure 7. The potential responses towards DCP and other interfering species were measured in 30 mM Tris buffer, pH 5. All of the phenols used in the selectivity test have pK_a values located within 7.89–13.6 range. This means that at pH 5, they will exist in their un-dissociated forms. The selectivity order for MIP/PANI membrane based sensor is: DCP > 2-chlorophenol > *p*-cresol > salicylate > phenol > bromide > chloride. The effect of PANI layer on the selectivity behavior of the sensor was also tested. The selectivity order for MIP membrane based sensor is: DCP > 2-chlorophenol > phenol > *p*-cresol > salicylate > bromide > acetate > formate > chloride. The selectivity order for neutral phenols is compatible with the lipophilicity in addition to the acidity of these phenols. As previously reported, a phenolic compound that possess high acidity and lipophilicity reveals a stronger super-Nernstian response with an anionic slope [45]. Acid dissociation constants in addition to partition coefficients of 2,4-DCP, 2-chlorophenol, *p*-cresol, salicylic acid and phenol are 7.89, 8.52, 10.3, 13.6 and 9.99, and 3.06, 2.15, 1.94, 2.26 and 1.46, respectively [46]. As noticed, 2,4-DCP has stronger acidity and higher lipophilicity over the other tested phenol derivatives. As shown in Table 1, the sensors revealed higher selectivity over all tested phenolic compounds and other inorganic anions and reflects the importance of using MIP beads as a recognition sensory element.

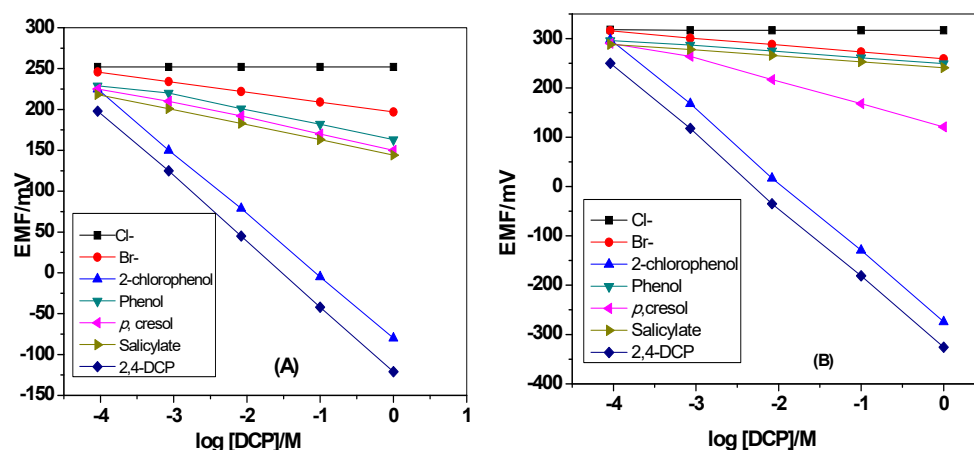


Figure 7. Potentiometric selectivity of MIP membrane-based sensors (A) with and (B) without polyaniline(PANI) as a solid-contact layer.

Table 1. Selectivity coefficients, $\text{Log } K^{pot}_{DCP,J}$, of the proposed screen-printed sensors.

Sensor	$\text{Log } K^{pot}_{DCP,J}$					
	Cl ⁻	Br ⁻	2-chlorophenol	phenol	p-cresol	salicylate
MIP	-10.8	-9.9	-0.8	-9.7	-7.5	-9.6
MIP+PANI	-6.3	-5.4	-0.7	-2.0	-4.4	-4.5

3.4. Constant-current Chronopotentiometry

Short-term potential stability was studied using chronopotentiometric methods. Figure 8 illustrates the typical chronopotentiogram of both MIP/PAN/-ISEs and MIP/ISEs for comparison. The potential drift ($\Delta E/\Delta t$) of MIP/PAN/-ISEs is $20.7 \pm 2.2 \mu\text{V/s}$ ($n = 3$), which is much lower than that of MIP/ISEs ($80.6 \pm 3.3 \mu\text{V/s}$) ($n = 3$). This indicates that the potential drift of the electrodes could be minimized by the introduction of PAN directly into the polymeric membrane. The redox capacitance for MIP/PAN/-ISEs is calculated to be $48.1 \pm 2.3 \mu\text{F}$ by using the equation $\Delta E/\Delta t = I/C$ [47]. For comparison, the estimated capacitance of MIP/ISEs was found to be $14.7 \pm 1.1 \mu\text{F}$. From the above results, we can correlate the relationship between the potential stability ($\Delta E/\Delta t$) or capacitance (C_L) and the presence of PAN as a solid contact material. The bulk resistance (R_b) of the MIP/ISEs and MIP/PANI/ISEs is found to be about 2.5 ± 0.7 and $0.75 \pm 0.08 \text{ M}\Omega$, respectively. The difference in total resistances can be explained as the result of PANI solubility in the membrane.

3.5. Electrochemical Impedances and Chronopotentiometry Measurements

The impedance plots for all-solid-state DCP-ISEs were shown in Figure 9. The bulk impedance of the membrane (R_b) and geometric capacitance (C_g) can be estimated from the high-frequency semicircle. The values of (R_b) and (C_g) were found to be ($R_b = 0.35 \text{ M}\Omega$, $C_g = 43.8 \pm 3.2 \text{ nF}$) and ($R_b = 6.0 \text{ M}\Omega$, $C_g = 29.2 \pm 2.1 \text{ nF}$) for MIP/PAN/-ISEs and MIP/ISEs, respectively. From the low-frequency branch (semicircle), which is characteristic for the type of solid contact used, the redox capacitance (C_L) is estimated. As shown in Figure 9b, the MIP/ISE presents large semicircle at the low-frequency range. This can be defined to the low capacitance and the high resistance at the “blocked” interface between the sensing membrane and the electronic conductor in the SPE platform. This can explain the long-term potential drift observed for MIP/ISE. For MIP/PAN-ISE, a depressed low-frequency semicircle is obtained and attributed to the presence of PANI layer which is responsible to ion-to-electron transduction through the interface located between the ISM and the conductive substrate. The low-frequency capacitance (C_L) for MIP/ISE and MIP/PAN-ISE were $C_L = 4.09 \pm 0.6 \mu\text{F}$ and $C_L = 10.8 \pm 1.1 \mu\text{F}$, respectively.

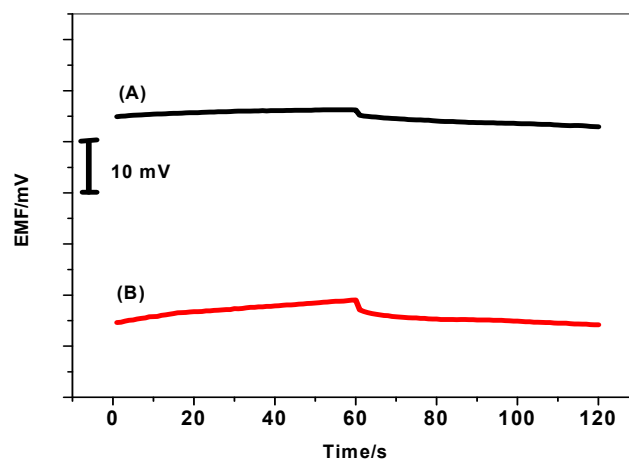


Figure 8. Chronopotentiometry for DCP/MIP-ISEs (A) with and (B) without PANI as a solid contact material.

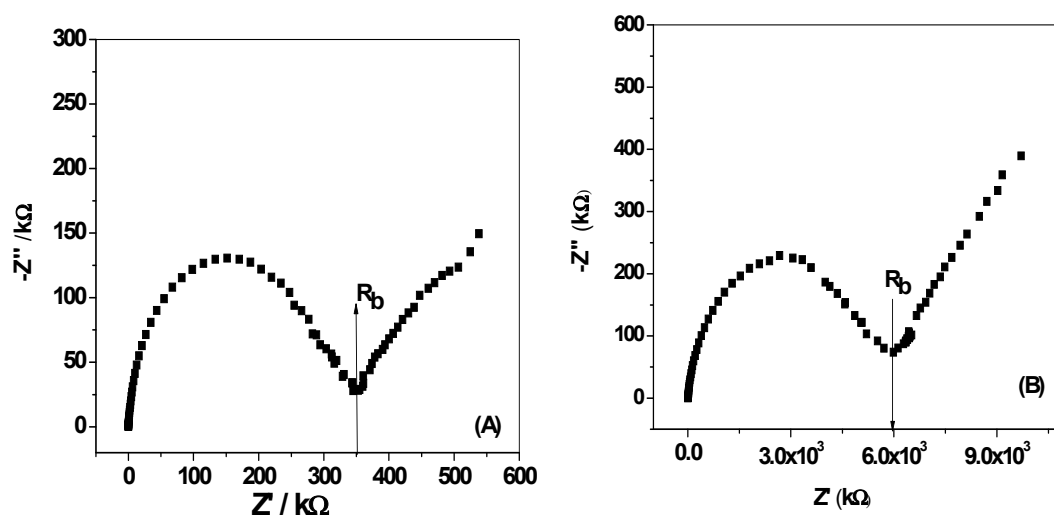


Figure 9. Impedance plot (A) for DCP/MIP-ISEs with and, (B) without PANI as a solid contact material.

3.6. Water Layer Test

The presence of water film at the interface between the ISM and the electronic conductive substrate can act as a localized microscopic pool of water [48]. It has a prejudicial effect to the potential stability and life time of the electrodes. Therefore, it is important to test the absence of this water layer in the presented ISEs in presence/absence of PANI layer. As shown in Figure 10, a stable potential was observed when MIP/PAN-ISE was immersed in Tris buffer. After the replacement of Tris buffer solution by 5.2 μm DCP solution, again stable potential is observed. After repeating the test with MIP/ISE, an immediate large potential shifts were recorded. It is obvious that a noticeable potential drift is recorded for MIP/ISE when changing back from tris buffer to 2,4-DCP. This indicates that a water film was formed between the ion sensing membrane and the electronic conductor. However, this drift is completely disappeared when using the PANI as the solid-contact layer. This demonstrates that the water layer was also eliminated by using the highly hydrophobic PANI layer.

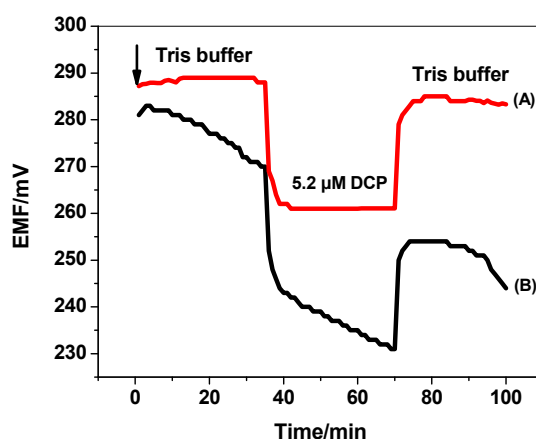


Figure 10. Water-layer tests for the DCP-ISE (A) with and (B) without PANI as the solid contact.

3.7. Analytical Applications

There are different causes for the presence of chlorophenols in drinking-water. They can be released in water as a result of the chlorination of phenols during disinfection. In addition, they can be produced as by-products after the reaction of phenols with hypochlorite or as degradation products of phenoxy herbicides. Chlorination increased the concentrations of 2-chlorophenol (2-CP), 2,4-dichlorophenol (2,4-DCP) and 2,4,6-trichlorophenol (2,4,6-TCP) [49]. The levels of chlorophenols in drinking-water are quite low and vary from one location to another. The maximum admissible level in water was regulated by the European union (EU) and US Environmental Protection Agency (EPA), and found to be 0.5 $\mu\text{g/L}$ [11]. The proposed MIP-based potentiometric sensor was introduced in a potentiometric setup and used to assess 2,4-DCP in different water samples collected from different places around Cairo, Egypt. The samples were then spiked with different concentration levels of 2,4-DCP and finally analyzed using the standard addition method. The accuracy was checked by measuring the recoveries of DCP in the water samples. The results were presented in Table 2. It can be seen that the recoveries of water samples vary from 95.8% to 108.3%. This can prove the feasibility of the proposed sensors for the assessment of 2,4-DCP in different complex samples.

Table 2. Application of the proposed sensor to determination of DCP in the water samples.

Sample	Proposed Sensor, (μM)*	Amount, μM *			HPLC, (μm) * [49]
		Added	Found	Recovery, (%)	
1	0.15 ± 0.06	0.5	0.67 ± 0.04	103.1	0.17 ± 0.06
2	0.22 ± 0.03	0.5	0.78 ± 0.07	108.3	0.21 ± 0.03
3	0.18 ± 0.02	0.5	0.65 ± 0.02	95.5	0.16 ± 0.02
4	0.31 ± 0.04	0.5	0.78 ± 0.08	96.2	0.35 ± 0.04
5	0.42 ± 0.03	0.5	0.95 ± 0.05	103.2	0.45 ± 0.03

* Average of three measurements \pm standard deviation.

4. Conclusions

Cost-effective and reliable disposable solid contact screen-printed electrodes based on uniform-sized MIP beads for 2,4-DCP detection have been presented. Polyaniline (PANI) was used as the ion to-electron transducer and showed excellent conductivity. The presented screen-printed platforms exhibited a rapid potential response towards 2,4-DCP in its neutral form with high selectivity over other phenol derivatives, in addition to high accuracy and precision. The overall presented method is precise, accurate, and inexpensive regarding reagent consumption and the equipment involved. The sensors were successfully applied to 2,4-DCP determination for concentration levels down to 0.4 μm .

Author Contributions: The listed authors contributed to this work as described in the following: S.E., A.H.K., and M.A.A. gave the concepts of the work, interoperated the results, the experimental part and prepared the manuscript, A.H.K. and S.E. cooperated in the preparation of the manuscript and A.H.K. and A.E.-G.E.A. performed the revision before submission. A.E.-G.E.A., M.A.A.-O. and N.M.K revealed the financial support for the work. All authors read and approved the final manuscript.

Funding: The authors are grateful to the Deanship of Scientific Research, King Saud University for funding this work through research group project “RGP-320”.

Conflicts of Interest: The authors declare no conflict of interest.

References

1. Sanchez-Prado, L.; Llompart, M.; Lores, M.; García-Jares, C.; Bayona, J.M.; Cela, R. Monitoring the photochemical degradation of triclosan in wastewater by UV light and sunlight using solid-phase micro extraction. *Chemosphere* **2006**, *65*, 1338–1347. [[CrossRef](#)] [[PubMed](#)]
2. Rule, K.L.; Ebbett, V.R.; Vikesland, P.J. Formation of chloroform and chlorinated organics by free-chlorine mediated chlorine mediated oxidation of triclosan. *Environ. Sci. Technol.* **2005**, *39*, 3176–3185. [[CrossRef](#)] [[PubMed](#)]
3. Hendricks, N.R.; Waryo, T.T.; Arotiba, O.; Jahed, N.; Baker, P.G.L.; Iwuoha, E.I. Microsomal cytochrome P450-3A4 (CYP3A4) nanobiosensor for the determination of 2,4-dichlorophenol-an endocrine disruptor compound. *Electrochim. Acta* **2009**, *54*, 1925–1931. [[CrossRef](#)]
4. Xu, Q.; Li, X.J.; Zhou, Y.E.; Wei, H.P.; Hu, X.Y.; Wang, Y.; Yang, Z.J. An enzymatic amplified system for the detection of 2,4-dichlorophenol based on graphene membrane modified electrode. *Anal. Methods* **2012**, *4*, 3429–3435. [[CrossRef](#)]
5. Huang, S.S.; Qu, Y.X.; Li, R.N.; Shen, J.; Zhu, L.W. Biosensor based on horseradish peroxidase modified carbon nanotubes for determination of 2,4-dichlorophenol. *Microchim. Acta* **2008**, *162*, 261–268. [[CrossRef](#)]
6. Makal, T.; Yakovenko, A.; Zhou, H. Isomerism in Metal–Organic Frameworks: “Framework Isomers”. *J. Phys. Chem. Lett.* **2011**, *2*, 1682–1689. [[CrossRef](#)]
7. Gui, B.; Meng, X.; Xu, H.; Wang, C. Postsynthetic Modification of Metal–Organic Frameworks through Click Chemistry. *Chin. J. Chem.* **2016**, *34*, 186–190. [[CrossRef](#)]
8. Wu, H.; Xia, B.; Yu, L.; Yu, X.; Lou, X. Porous molybdenum carbide nano-octahedrons synthesized via confined carburization in metal-organic frameworks for efficient hydrogen production. *Nat. Commun.* **2015**, *6*, 6512–6519. [[CrossRef](#)]
9. He, H.; Song, Y.; Sun, F.; Bian, Z.; Gao, L.; Zhu, G. A porous metal–organic framework formed by a V-shaped ligand and Zn(II) ion with highly selective sensing for nitroaromatic explosives. *J. Mater. Chem. A* **2015**, *3*, 16598–16603. [[CrossRef](#)]
10. Zubair, H.; Hwa, J. Removal of hazardous organics from water using metal-organic frameworks (MOFs): Plausible mechanisms for selective adsorptions. *J. Hazard. Mater.* **2015**, *283*, 329–339.
11. Pera-Titus, M.; García-Molina, V.; Baños, M.A.; Giménez, J.; Esplugas, S. Degradation of chlorophenols by means of advanced oxidation processes: A general review. *Appl. Catal. B Environ.* **2004**, *47*, 219–256. [[CrossRef](#)]
12. Zheng, C.; Zhao, J.; Bao, P.; Gao, J.; He, J. Dispersive liquid–liquid microextraction based on solidification of floating organic droplet followed by high-performance liquid chromatography with ultraviolet detection and liquid chromatography–tandem mass spectrometry for the determination of triclosan and 2,4-dichlorophenol in water samples. *J. Chromatogr. A* **2011**, *1218*, 3830–3836. [[PubMed](#)]
13. Holopainen, S.; Luukkonen, V.; Nousiainen, M.; Sillanpää, M. Determination of chlorophenols in water by headspace solid phase microextraction ion mobility spectrometry (HS-SPME-IMS). *Talanta* **2013**, *114*, 176–182. [[CrossRef](#)] [[PubMed](#)]
14. Guo, L.; Lee, H.K. Electro membrane extraction followed by low-density solvent based ultrasound-assisted emulsification microextraction combined with derivatization for determining chlorophenols and analysis by gas chromatography–mass spectrometry. *J. Chromatogr. A* **2012**, *1243*, 14–22. [[CrossRef](#)] [[PubMed](#)]
15. Hallaj, T.; Amjadi, M. Determination of 2,4-dichlorophenol in water samples using a chemiluminescence system consisting of graphene quantum dots, rhodamine B and cerium(IV) ion. *Microchim. Acta* **2016**, *183*, 1219–1225. [[CrossRef](#)]

16. Hassan, S.S.M.; Abdel-Shafi, A.A.; Mohammed, A.H.K. Flow injection fluorimetric determination of chromium (VI) in electroplating baths by luminescence quenching of tris(2,2'-bipyridyl) ruthenium(II). *Talanta* **2005**, *67*, 696–702. [[CrossRef](#)]
17. Zhang, L.H.; Zhang, C.J.; Chen, X.; Feng, Y.Q.; Wu, X.Z. In-capillary solid-phase extraction capillary electrophoresis for the determination of chlorophenols in water. *Electrophoresis* **2006**, *27*, 3224–3232. [[CrossRef](#)]
18. Rama, M.J.R.; Medina, A.R.; Díaz, A.M. A simple and straightforward procedure for monitoring phenol compounds in waters by using UV solid phase transduction integrated in a continuous flow system. *Microchim. Acta* **2003**, *141*, 143–148. [[CrossRef](#)]
19. Miao, J.; Li, D.; Ran, Y.; Qu, L.; Harrington, P.D.B. Synthesis of poly(sodium 4-styrenesulfonate) functionalized graphene/cetyltrimethylammonium bromide (CTAB) nanocomposite and its application in electrochemical oxidation of 2,4-dichlorophenol. *Electrochim. Acta* **2014**, *125*, 1–8.
20. Whitcombe, M.J.; Kirsch, N.; Nicholls, I.A. Molecular imprinting science and technology: A survey of the literature for the years 2004–2011. *J. Mol. Recognit.* **2014**, *27*, 297–401.
21. Dabrowski, M.; Lach, P.; Ceiplak, M.; Kutner, W. Nanostructured molecularly imprinted polymers for protein chemsensing. *Biosens. Bioelect.* **2018**, *102*, 17–26. [[CrossRef](#)] [[PubMed](#)]
22. Kutner, W.; Sharma, S.P. *Molecularly Imprinted Polymers for Analytical Applications*; The Royal Society of Chemistry (RSC): London, UK, 2018.
23. Kupai, J.; Razali, M.; Buyuktiryaki, S.; Kecili, R.; Szekely, G. Long-term stability and reusability of molecularly imprinted polymers. *Polym. Chem.* **2017**, *8*, 666–673. [[CrossRef](#)] [[PubMed](#)]
24. El-Kosasy, A.M.; Kamel, A.H.; Hussin, L.A.; Ayad, M.F.; Fares, N.V. Mimicking new receptors based on molecular imprinting and their application to potentiometric assessment of 2,4-dichlorophenol as a food taint. *Food Chem.* **2018**, *250*, 188–196. [[CrossRef](#)] [[PubMed](#)]
25. Kamel, A.H.; Mohammad, S.G.; Awwad, N.S.; Mohammed, Y.Y. Survey on the Integration of Molecularly Imprinted Polymers as Artificial Receptors in Potentiometric Transducers for pharmaceutical Drugs. *Int. J. Electrochem. Sci.* **2019**, *14*, 2085–2124. [[CrossRef](#)]
26. El-Naby, E.H.; Kamel, A.H. Potential transducers based man-tailored biomimetic sensors for selective recognition of dextromethorphan as an antitussive drug. *Mat. Sci. Eng. C* **2015**, *54*, 217–224. [[CrossRef](#)] [[PubMed](#)]
27. El-Shalakany, H.H.; Hamza, M.S.A.; Kamel, A.H. Solid-contact potentiometric sensors for reliable automatic quantification of 2,4-dichlorophenol (2,4-DCP) as a food taint. *Meas. Sci. Technol.* **2018**, *29*, 105102. [[CrossRef](#)]
28. Wang, T.; Liang, R.; Yin, T.; Yao, R.; Qin, W. An all-solid-state imprinted polymer-based potentiometric sensor for determination of bisphenol S. *RSC Adv.* **2016**, *6*, 73308–73312. [[CrossRef](#)]
29. Bobacka, J.; Lindfore, T.; McCarrick, M.; Ivaska, A.; Lewenstam, A. Single-Piece All-Solid-State Ion-Selective Electrode. *Anal. Chem.* **1995**, *67*, 3819–3823. [[CrossRef](#)]
30. Cattrall, R.W.; Preiser, H. Coated wire ion-selective electrodes. *Anal. Chem.* **1971**, *43*, 1905–1906. [[CrossRef](#)]
31. Cattrall, R.W.; Hamilton, I.C. Coated-wire ion-selective electrodes. *Ion-Sel. Electrode Rev.* **1984**, *6*, 125–172.
32. Bobacka, J. Conducting polymer-based solid-state ion-selective electrodes. *Electroanalysis* **2010**, *18*, 7–18. [[CrossRef](#)]
33. Bobacka, J.; Ivaska, A.; Lewenstam, A. Potentiometric ion sensors. *Chem. Rev.* **2008**, *108*, 329–351. [[CrossRef](#)] [[PubMed](#)]
34. Hu', J.B.; Stein, A.; Buhlmann, P. Rational design of all-solid-state ion-selective electrodes and reference electrodes. *TrAC Trends Anal. Chem.* **2016**, *76*, 102–114.
35. Jaworska, E.; Mazur, M.; Maksymiuk, K.; Michalska, A. The fate of poly(3-octylthiophene) transducer in solid contact ion-selective electrodes. *Anal. Chem.* **2018**, *90*, 2625–2630. [[CrossRef](#)] [[PubMed](#)]
36. Paczosa-Bator, B.; Cabaj, L.; Ras, M.; Bas, B.; Piech, R. Potentiometric sensor platform based on a carbon black modified electrodes. *Int. J. Electrochem. Sci.* **2014**, *9*, 2816–2823.
37. Crespo, G.A.; Macho, S.; Rius, F.X. Ion-selective electrodes using carbon nanotubes as ion-to-electron transducers. *Anal. Chem.* **2008**, *80*, 1316–1322. [[CrossRef](#)] [[PubMed](#)]
38. Ping, J.F.; Wang, Y.X.; Wu, J.; Ying, Y.B. Development of an all-solid-state potassium ion-selective electrode using graphene as the solid-contact transducer. *Electrochem. Commun.* **2011**, *13*, 1529–1532. [[CrossRef](#)]
39. Hu, J.B.; Zou, X.U.; Stein, A.; Buhlmann, P. Ion-selective electrodes with colloid-imprinted mesoporous carbon as solid contact. *Anal. Chem.* **2014**, *86*, 7111–7118. [[CrossRef](#)]

40. Cuartero, M.; del Rio, J.S.; Blondeau, P.; Ortuno, J.A.; Rius, F.X.; Andrade, F.J. Rubber-based substrates modified with carbon nanotubes inks to build flexible electrochemical sensors. *Anal. Chim. Acta* **2014**, *827*, 95–102. [[CrossRef](#)]
41. An, Q.; Jiao, L.; Jia, F.; Ye, J.; Li, F.; Gan, S.; Zhang, Q.; Ivaska, A.; Niu, L. Robust single-piece all-solid-state potassium-selective electrode with monolayer-protected Au clusters. *J. Electroanal. Chem.* **2016**, *781*, 272–277. [[CrossRef](#)]
42. Yoshimatsu, K.; Reimhult, K.; Krozer, A.; Mosbach, K.; Sode, K.; Ye, L. Uniform molecularly imprinted microspheres and nanoparticles prepared by precipitation polymerization: The control of particle size suitable for different analytical applications. *Anal. Chim. Acta* **2007**, *584*, 112–121. [[CrossRef](#)] [[PubMed](#)]
43. Bakker, E. Determination of Unbiased Selectivity Coefficients of Neutral Carrier-Based Cation-Selective Electrodes. *Anal. Chem.* **1997**, *69*, 1061–1069. [[CrossRef](#)]
44. Liang, R.N.; Kou, L.J.; Chen, Z.P.; Qin, W. Molecularly imprinted nanoparticles based potentiometric sensor with a nanomolar detection limit. *Sens. Actuators B* **2013**, *188*, 972–977. [[CrossRef](#)]
45. Ito, T.; Radecka, H.; Tohda, K.; Odashima, K.; Umezawa, Y. On the Mechanism of Unexpected Potentiometric Response to Neutral Phenols by Liquid Membranes Based on Quaternary Ammonium Salts-Systematic Experimental and Theoretical Approaches. *J. Am. Chem. Soc.* **1998**, *120*, 3049–3059. [[CrossRef](#)]
46. PubChem. Available online: <https://pubchem.ncbi.nlm.nih.gov> (accessed on 11 August 2019).
47. Bobacka, J. Potential stability of all-solid-state ion-selective electrodes using conducting polymers as ion-to-electron transducers. *Anal. Chem.* **1999**, *71*, 4932–4937. [[CrossRef](#)] [[PubMed](#)]
48. Veder, J.; De Marco, R.; Clarke, G.; Chester, R.; Nelson, a.; Prince, K.; Pretsch, E.; Bakker, E. Elimination of undesirable water layers in solid-contact polymeric ion-selective electrodes. *Anal. Chem.* **2008**, *80*, 6731–6740. [[CrossRef](#)] [[PubMed](#)]
49. World Health Organization. *Guidelines for Drinking-Water Quality*, 2nd ed.; World Health Organization: Geneva, Switzerland, 1996; Volume 2.



© 2019 by the authors. Licensee MDPI, Basel, Switzerland. This article is an open access article distributed under the terms and conditions of the Creative Commons Attribution (CC BY) license (<http://creativecommons.org/licenses/by/4.0/>).